Cation Sensors Based on Terpyridine-Functionalized Boradiazaindacene

Christine Goze,[a] Gilles Ulrich,[a] Loïc Charbonnière,[a] Michèle Cesario,[b] Thierry Prangé,[c] and Raymond Ziessel*[a]

Abstract: A new class of highly luminescent dyes is reported. The characteristic feature of these compounds is that a terpyridine fragment is closely appended to a boradiazaindacene moiety in such a way that cation binding to the vacant terpyridine causes strong perturbations of the photophysical properties of the boradiazaindacene unit. In particular, these sensors are especially applicable to the fluorescence detection of trace quantities of zinc(II) ions in solution. The mechanism of the cation-induced quenching process has been investigated by a combination of electrochemistry, UV/Vis absorption, emission, and NMR spectroscopy. Highly luminescent arrays can be formed by doping transparent polymers with low concentrations of these new dyes. In such materials, the change in photophysical properties upon cation binding is so marked that "cation writing" becomes feasible under routine conditions.

Keywords: detectors · luminescence · N ligands · polymers · triethylenetetramine

Introduction

Highly luminescent materials have attracted considerable attention over the past few decades, boosted by potential applications in medical diagnostics, molecular biology, molecular recognition, and material science.[1–4] Many elegant scaffolds, such as preorganized molecular pockets,[5, 6] fluorescent tweezers,[7] and molecular beacons[8] have been investigated in an attempt to identify alternative ways for effective detection of those charged species, saccharides, or oligonucleotides that play a fundamental role in biological and environmental processes. Most of the systems developed to date use optical variations as the output signal, and in some cases the transduction process is rather efficient.[8] While organic chromophores dominate the field, there is intense interest in designing alternative systems bearing disparate functions (e.g., photo- or electroactivity) or recognition sites and possessing easily modified organic shells. We have focused our investigations on ruthenium[9] and lanthanide[10] complexes for which fine-tuning of the electronic properties allows us to detect certain cations or anions in solution. Usually, the binding event is monitored by changes in the absorption and fluorescence intensity. Unfortunately, the performance of these systems has been limited by a range of factors, not least of which is the modest variation in emission yield upon substrate binding and light dissipation due to detrimental non-radiative deactivation pathways. Recently, a new class of chromogenic reagents for optical detection was discovered. These compounds highlight the advantage of using a hybrid approach in which the chromophore is directly linked to the complexation pocket.[11, 12]

Herein, we describe the concept of attaching a very efficient fluorescence reporter, which is based on a 4,4-difluoro-4-bora-3a,4a-diaza-*s*-indacene (BODIPY) chromophore, to a 2,2′:6′,2″-terpyridine (terpy) fragment. The overall intention has been to produce molecular sensors that can be monitored physically or chemically and that respond to added cations. These novel ligands are termed BODITERPY. The choice of 2,4-dimethyl-3-ethylpyrrole (Kryptopyrrol)[13] was motivated for synthetic reasons and by the fact that such materials usually impart high fluorescence quantum yields to the subsequent conjugate,[14] while terpy subunits are known to be excellent cation binders.

Results and Discussion

The novel BODITERPY dyes **1** and **2** where prepared according to Scheme 1 and unambigously characterized by mass spectrometry and elemental analysis [FAB$^+$ *m*/*z*, *m*-

[a] Dr. R. Ziessel, C. Goze, Dr. G. Ulrich, Dr. L. Charbonnière
Laboratoire de Chimie Moléculaire
Associé ou CNRS, ECPM
25 rue Becquerel, 67087 Strasbourg Cedex 02 (France)
Fax: (+33) 3 90 24 26 89
E-mail: ziessel@chimie.u-strasbg.fr

[b] Dr. M. Cesario
Institut de Chimie des Substances Naturelles
CNRS, 91128 Gif-sur-Yvette (France)

[c] Dr. T. Prangé
LURE Bât. 209d
Université Paris-Sud, 91405 Orsay (France)

Supporting information for this article is available on the WWW under http://www.chemeurj.org or from the author: UV/Vis spectra and titration experiments of ligand **1** and **2** with all cations are provided.

DOI: 10.1002/chem.200305084

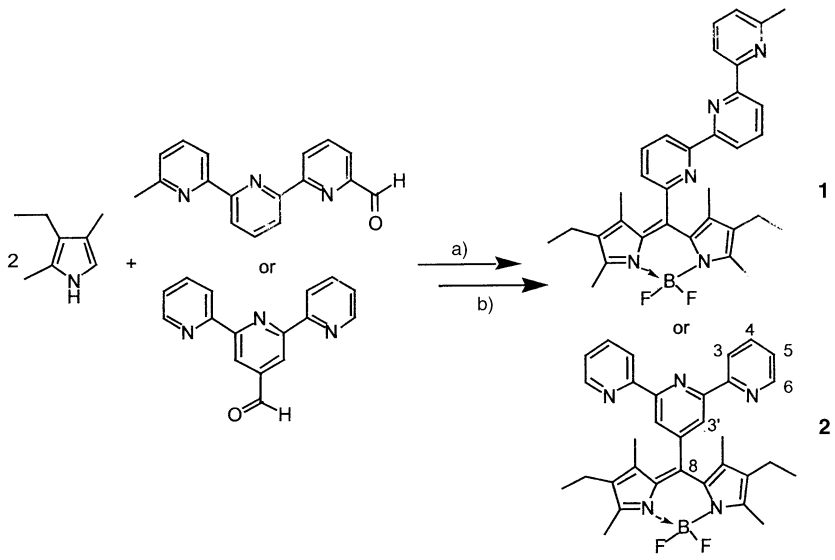

Scheme 1. a) TFA cat., DDQ (1 equiv), CH_2Cl_2, RT; b) TEA, $BF_3 \cdot Et_2O$, toluene, 100 °C. Overall yield 8% for **1** and 73% for **2**. TFA = trifluroacetic acid, DDQ = 2,3-dichloro-5,6-cyano-1,4-benzoquinone, TEA = triethylamine.

NBA, 550.3 (100, [M^++H]) for **1** and 536.2 for **2** (100, [M^++H])]. Both ligands exhibit well-defined ^{1}H, ^{11}B, and ^{13}C NMR spectra, while full assignment of the protons was realized by way of 2D COSY ans NOESY experiments. The absence of dipolar correlation between vicinal pyridine rings strongly supports the idea of a *trans* conformation for the pyridine rings of both free ligands. On the basis of symmetry considerations, C_s and C_{2v} point groups for **1** and **2**, respectively, it was concluded that the terpy and indacene mean planes are orthogonal in solution.

Abstract in French: *Une nouvelle famille de pigments extrêmement fluorescents comportant une partie chélatante de type terpyridine connectée de façon covalente à une entité boradiazaindacene a été synthétisée et caractérisée. La complexation de cations comme le zinc, le magnésium et le strontium par le site terpyridinique perturbe les propriétés optiques et, en particulier, la luminescence de la sonde boradiazaindacene. La seule complexation d'un équivalent de zinc divalent engendre une diminution de la fluorescence de plus de 90 %. Cette observation permet de détecter des traces de zinc à hauteur de 40 ppb. Les constantes d'association et la stoechiométrie des différentes espèces ont été déterminées par dosage spectrophotométrique et par luminescence dans le cas du zinc. La phénoménologie du processus d'extinction de luminescence a été étudiée par une combinaison d'études électrochimiques et photophysiques ainsi qu'avec des études de RMN en solution. La réversibilité du phénomène et la stabilité des nouvelles molécules a été démontrée en solution diluée. De plus, le dopage de polymères transparents de type polymétacrylate avec ces nouveaux fluorophores permet d'écrire au travers d'un pochoir et d'effacer cette écriture avec un compétiteur du zinc. Ces observations sont faites par luminescence à des longueurs d'ondes standard. Le potentiel de cette nouvelle approche conceptuelle a été évaluée en guise de conclusion.*

The X-ray structure determination of ligand **1** (Figure 1a) confirmed the orthogonal placement of the terpy and dipyrrolic fragments and that the molecule is sterically congested. The dihedral angles of 6.5(1)° between the planes of the rings containing the N1A and N1B nitrogen atoms and 2.9(2)° between the planes of the rings containing N1A and N1C nitrogen atoms, respectively, illustrate the twist about the interannular C–C bond. There is slight distortion within the terpy unit, which is evidenced by the dihedral angle of 8.3(2)° between the pyridino N1B and N1C nitrogen atoms. As surmised from the results of the NMR studies, all three nitrogen atoms of the terpy moiety lie in a transoidal arrangement that minimizes electrostatic interactions between the neighboring lone pairs, a situation frequently found in oligopyridine ligands. Interestingly, the indacene fragment is almost planar (the maximum deviation from the least-squares mean plane of the 12 atoms of the indacene group is 0.081(2) Å) and perpendicular to the mean plane defined by the chelate (tilt angle of 89.48(7)°). A striking result revealed by the crystal packing is the cofacial arrangement of two molecules caused by $\pi-\pi$ stacking of two centrosymmetrical pyridine rings held apart at an average distance of 3.8 Å. Furthermore, the pyridine ring $(0.5+x, -0.5-y, -0.5+z)$ not involved in this intermolecular interaction is almost orthogonal (83°) to the central pyridine $(-x, -y, -z)$ ring of a neighboring molecule located at a distance of 3.35 Å (Figure 1b).

Electronic absorption spectra recorded for the new ligands show the expected features of the constituent BODIPY and terpy moieties (Figures S1 and S2 in the Supporting Information). Both dyes emit around 550 nm with high fluorescence quantum yields. Spectroscopic and redox data are collected in Table 1. In general, the Stokes' shift ($\Delta\nu \approx 800$ cm^{-1}) and the short excited singlet state lifetime found for both **1** and **2** are in keeping with results found for related BODIPY dyes.[15] The absorption and the emission maxima are essentially independent of solvent polarity, indicating that there is no significant change in dipole moment upon excitation. This finding, in turn, implies that the observed fluorescence is localized on the BODIPY unit and does not arise as a result of intramolecular charge transfer. More interestingly, progressive addition of trace amounts of cations resulted in an "on/off switching" of the luminescence intensity. Presumably, this latter effect is associated with coordination at the terpy subunit (Figure 2).

To examine more closely the chelating ability of these ligands, UV/Vis titrations were carried out in acetonitrile for increasing quantities of cations. The results are gathered in

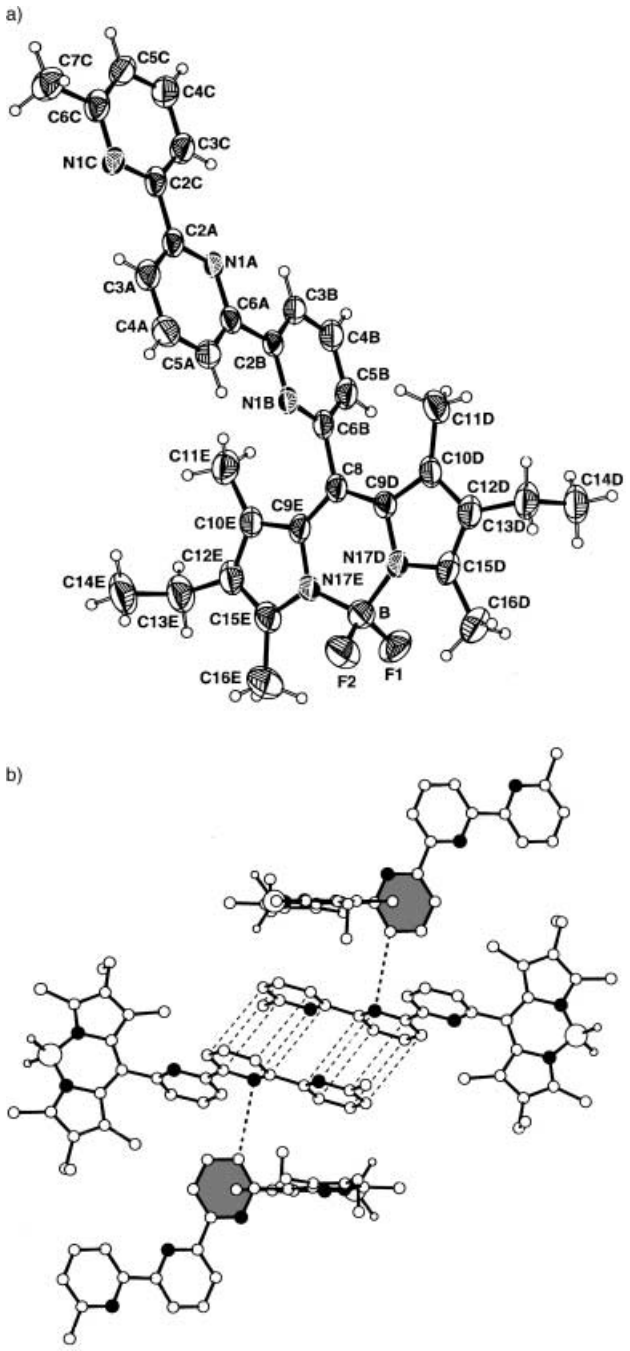

Figure 1. a) Structure of **1** (with displacement ellipsoids drawn at 50% probability level and H atoms shown as small spheres of arbitrary radii). b) Illustration of the significant role played by $\pi-\pi$ stacking interactions in the crystal structure of ligand **1**.

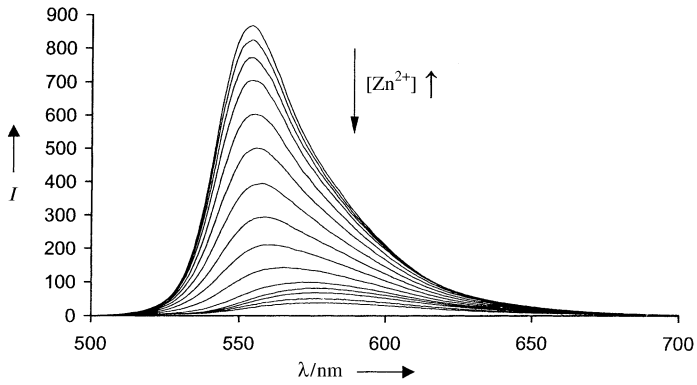

Figure 2. Overlay of luminescence spectra recorded during the titration of **2** with Zn^{2+} ions in CH_3CN at 20 °C, showing the progressive decrease in intensity and red shift noted for the emission peak on coordination of the cation to the vacant site on terpyridine.

Table 2 and in all cases, the absorption spectra clearly show a bathochromic shift of the main absorption band at 280 nm upon addition of the cation, with a concomitant appearance of

Table 2. Cumulative stability constants for complexation of **1** and **2** with various cations (added as their hydrated perchlorate salts) in acetonitrile (0.01 M $TBAPF_6$, 298 K).

M^{n+}	L	$\log\beta_{11}$	$\log\beta'_{11}$[a]	$\log\beta_{12}$	$\log\beta'_{12}$[a]
Zn^{2+}[b]	**1**	8.4 ± 0.5	–	14.8 ± 0.5	–
Zn^{2+}[c]	**2**	8.2 ± 0.5	7.4 ± 0.4	14.3 ± 0.7	12.3 ± 0.5
Mg^{2+}	**2**	6.3 ± 0.2	–	11.8 ± 0.4	–
Ca^{2+}	**2**	6.6 ± 0.4	–	12.5 ± 0.6	–
Sr^{2+}[d]	**2**	6.4 ± 0.3	–	11.3 ± 0.2	–

[a] Determined by fluorescence spectroscopy over two different titrations, $\lambda_{exc}=316$ nm. [b] An additional $[M_2L_3]$ species was evidenced with $\log\beta_{23}=29.0\pm0.7$. [c] Average value taken over four different titrations performed by direct addition of the cation to a ligand solution (three times), and one reversed addition. [d] An additional $[ML_3]$ species was found with $\log\beta_{13}=16.4\pm0.2$.

a new band centered around 310 nm (Figure 3). The band at 280 nm is attributed to a mixture of $\pi\rightarrow\pi^*$ and $n\rightarrow\pi^*$ transitions localized on the terpy unit, and the bathochromic shift is a clear indication that complexation involves this part of the molecule.[16] A less pronounced bathochromic shift of the absorption band at 518 nm was also observed (Figure 3). This absorption transition corresponds to population of the first singlet excited state centered on the BODIPY fragment.[17] The observed spectral shift is attributed to a combination of conformational changes and electronic per-

Table 1. Spectroscopic[a] and redox[b] data for the two ligands at 298 K.

Compound	λ_{abs} [nm]	ε_{max} [$M^{-1}cm^{-1}$]	λ_F [nm]	ϕ_F[c] [%]	τ_F [ns]	k_r[d] [$10^8\ s^{-1}$]	k_{nr}[d] [$10^7\ s^{-1}$]	E_{oxy} (δE_p) [V] ([mV])	E_{red} (E_p) [V] ([mV])
1	529	67000	552	56	4.8	1.17	9.17	+1.02 (60)	−1.22 (72)
2	529	72000	548	87	5.3	1.65	2.45	+1.11 (70)	−1.14 (60), −1.74 (70)

[a] Determined in dichloromethane: 2.8×10^{-5} M for **1** and 1.8×10^{-5} M for **2**, $\lambda_{exc}=529$ nm. [b] Potentials determined by cyclic voltammetry in deoxygenated acetonitrile solution containing 0.1 M $TBAPF_6$ at a solute concentration of 1.5×10^{-3} M. Potentials were standardized by using ferrocene (Fc) as internal reference and converted to SSCE assuming that $E_{1/2}$ (Fc/Fc^+) = 0.37 V versus SSCE. All redox events are monoelectronic. Error on all half-wave potentials is ±10 mV. [c] Determined in dichloromethane: 3.2×10^{-7} M for **1** and 4.5×10^{-7} M for **2**. Using Rhodamine 6G as reference $\phi_F=0.76$ in water, $\lambda_{exc}=488$ nm.[21] All ϕ_F are corrected for changes in refractive index. [d] Calculated by using the following equations: $k_r=\phi_F/\tau_F$, $k_{nr}=(1-\phi_F)/\tau_F$, assuming that the emitting state is produced with unit quantum efficiency.

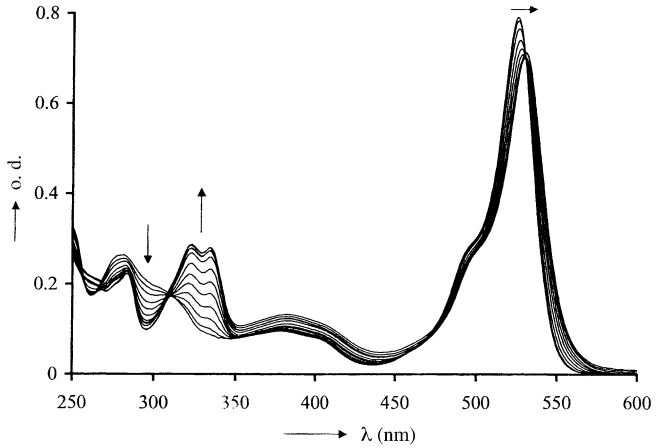

Figure 3. Evolution of the UV/Vis absorption spectra of a solution of **2** upon addition of increasing amounts of zinc(II) perchlorate in CH_3CN, 0.01M $TBAPF_6$ (corrected for dilution).

turbations associated with complexation at the terpy unit. That the two subunits interact was apparent from the results of a ^1H NMR titration study carried out with **2**; pronounced NOE effects were found between the neighboring H3 and H3′ protons of the terpy core and between H3′ and the methyl groups of the indacene subunit.

For Zn^{2+}, Mg^{2+}, Ca^{2+}, and Sr^{2+} ions, analysis of the UV/Vis spectrophotometric titration data with ligand **2** required the presence of two major components and lead to the formation of the cation complexes. This behavior is interpreted in that complexation involves both 1:1 and 1:2 cation/ligand stoichiometries (Table 2). From the titration of Zn^{2+} ions with ligand **2**, the evolution of the spectra was fitted to a mathematical model that includes these two species and which allows the calculation of their concentrations (Figure 4). The absorption spectra of the new species were reconstituted as sketched in Figure 5. These data confirm the bathochromic shift of the singlet transition and of the π–π* absorption band of the terpy moieties. As expected, Zn^{II} ions display the strongest affinity for the ligand, as evidenced

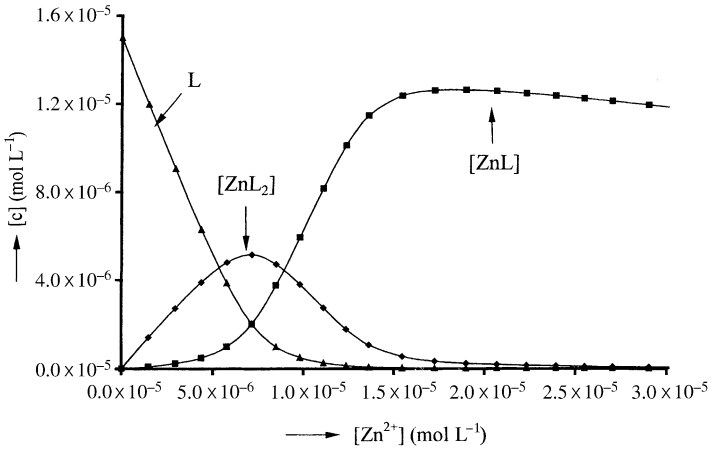

Figure 4. Calculated concentrations of the species observed during the titration of **2** with zinc(II) perchlorate in CH_3CN, 0.01M $TBAPF_6$ (uncorrected for dilution).

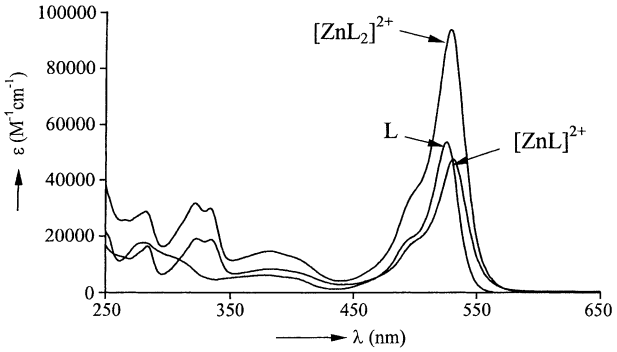

Figure 5. Calculated absorption spectra of the species observed during the titration of **2** with zinc(II) perchlorate in CH_3CN, 0.01M $TBAPF_6$.

by the derived stability constants. With the alkaline-earth metals, the ML complexes are two orders of magnitude less stable than for the corresponding Zn^{II} complexes and no significant selectivity could be observed on moving down the series from Mg^{2+} to Sr^{2+}. In the case of the bigger strontium ion, an additional ML_3 species was observed in the presence of a large excess of the ligand. Interestingly, in the case of the monovalent cations K^+, Na^+, Li^+, NH_4^+, and the tetraalkylammonium ions R_4N^+, complexation is too weak to cause significant perturbation of either the UV/Vis absorption spectrum or the visible fluorescence spectrum. Similarly, no effect could be detected upon addition of CF_3COOH in acetonitrile.

In the case of Zn^{II} ions, there is a clear isosbestic point at 316 nm that can be used to simplify analysis of the corresponding fluorescence titrations. Thus, values obtained by fluorescence spectroscopy for the stepwise complexation of Zn^{2+} to **2** are in good agreement to those obtained by absorption spectroscopy (Table 2). For ligand **2**, the addition of one equivalent of Zn^{2+} results in the loss of 90% of the initial luminescence intensity (Figure 2). This is a useful finding because, when taken with the high fluorescence yield found in the absence of cation, it allows detection of Zn^{II} ions at low concentration (lower limit is ca. 40 ppb).[18] Complete recovery of the fluorescence signal is observed upon addition of a competing ligand such as triethylenetetraamine (Figure 6). At least three full cycles can be performed without degradation of the dye.

UV/Vis titration experiments with ligand **1** and Zn^{2+} pointed to the presence of an additional species with a M_2L_3 formulation, which was corroborated by ^1H NMR titration experiments. The presence of up to three new species in solution renders the interpretation of the quenching process hazardous.

Both BODITERPY ligands exhibit well-defined, quasi-reversible oxidation of the indacene to the radical cation, although **1** is easier to oxidize by 90 mV due to the combined electron-donating effect of the terpy substituents and to the substitution pattern. This electronic effect is also reflected in the cathodic part of the voltamogram which shows that the indacene radical anion in ligand **2** is easier to obtain by about 80 mV than that in ligand **1** (Table 1). Interestingly, stepwise addition of **2** (in portions corresponding to 0.5 equiv) to a solution of anhydrous $Zn(OTf)_2$ resulted in the formation of

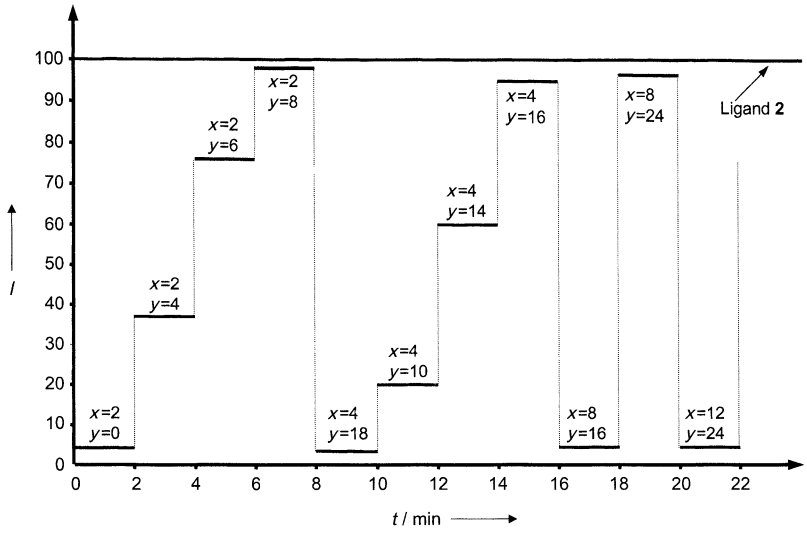

Figure 6. The upper curve shows the fluorescence intensity I recorded as a function of time t for 1.7 μM of ligand **2** in acetonitrile under aerobic conditions at 20 °C; x corresponds to the number of added equivalents of $Zn(ClO_4)_2 \cdot 6H_2O$ and y corresponds to the number of equivalents of triethylenetetramine added. The slot times are two minutes in each case and the values are corrected for minor effects of dilution.

[Zn(**2**)] and [Zn(**2**)$_2$]; the two complexes show marked different electrochemical properties. For both complexes, the indacene radical anion is formed at a potential that is 240 mV less negative than that of the free ligand **2**. However, the most spectacular changes are found for the first reduction of the terpy fragment which occurs at -1.41 V ($\Delta E_p = 60$ mV) and -0.96 V ($\Delta E_p = 60$ mV) for [Zn(**2**)] and [Zn(**2**)$_2$], respectively, Both potentials are markedly less cathodic than needed for reduction of the terpy fragment in the free ligand, reflecting the inductive effect of the cation. It is noteworthy that the free ligand and the two cation complexes exhibit a quasi-reversible oxidation peak at $+1.11$ V ($\Delta E_p = 70$ mV), which is attributed to oxidation of the indacene unit (under the same conditions an authentic sample of [Zn(terpy)$_2$] showed no oxidation peaks).

These electrochemical results permit a discussion of the possible light-induced electron transfer processes that might be anticipated to take place within the various zinc(II) complexes. Thus, taking into account the first oxidation process in [Zn(**2**)] and the energy required to populate the first singlet excited state ($E_{00} \approx 2.3$ eV), the oxidation potential for this excited singlet state can be approximated as $E_{2^+/2^*} \approx -1.19$ V. Bearing in mind that the first terpy-based reduction of the [Zn(**2**)] complex occurs at -1.41 V it follows that an oxidative photoinduced electron transfer from the indacene unit to the adjacent (Zn–terpy) fragment is thermodynamically unfavorable. The same calculation for [Zn(**2**)$_2$] indicates that light-induced electron transfer within the complex is thermodynamically favored by about 230 mV. We should note, however, that formation of the 1:2 complexes causes only a modest decrease in the fluorescence intensity relative to that of the 1:1 complex.

The mechanism by which cation complexation causes extinction of fluorescence from the BODIPY fragment is not yet clear. Fluorescence from the Zn–terpy unit[19] in [Zn(**2**)] can be detected at around 365 nm and this emission is much less intense in [Zn(**2**)$_2$], when excited at 315 nm. It is likely that singlet–singlet energy transfer decreased from the Zn–terpy unit to the nearby BODIPY fragment but this is not sufficient to explain the observed decrease in fluorescence from the indacene part of the molecule. For instance, direct excitation of the indacene singlet at 529 nm while adding increasing amounts of zinc results in a similar quenching phenomenon. Low-temperature steady-state emission studies recorded in an EtOH/CH_3OH 4:1 glass at 77 K did not detect a low-lying excited state originating from a spin-orbit coupling.[20] Thus, additional studies are needed to elucidate the quenching mechanism.

Finally, the marked change in fluorescence intensity found between BODITERPY and its zinc(II) complex provides the basis for fluoroimaging. To test this possiblity a poly(methylmethacrylate) polymer film ($M_w = 95\,000$, $M_n = 65\,000$) was doped with **2** (0.5 % wt) to produce a highly fluorescent plastic material that could be shaped at will (Figure 7a). Exposure of this film through a shadow mask to a solution of a zinc(II) salt caused the appearance of a red non-luminescent image on the green luminescent background (Figure 7b). This nonluminescent image is extremely stable (over ten months up to now), and could be transferred to a conductive support or reversibly erased by treatment with a zinc competitor. Interestingly, this positive image could be erased by spraying in a second step triethylenetetramine in acetonitrile. As shown in Figure 7c, the luminescence of the dye is restored and the zinc image is implicit. Control experiments carried out with compounds lacking the terpy subunit but carrying a toluyl fragment (Figure 7d), revealed no significant change in the brightness of the fluorescence upon exposure to the cation (Figure 7e). Further examination of these systems are underway in our laboratory to provide spatially controlled microstructures in the dimension perpendicular to the underlying substrate.

Experimental Section

General: CH_2Cl_2 and toluene were distilled over P_2O_5 and sodium, respectively, prior to use. 4′-Formyl-2′:2″;6″:2‴terpyridine was synthesized according to reference [22]. The 200 (^{1}H), 50.3 (^{13}C), and 128.4 (^{11}B) MHz NMR spectra were recorded at room temperature on a Bruker AC 200 spectrometer (^{1}H, ^{13}C) or Bruker 400 avance series spectrometer (^{11}B). FTIR spectra were recorded as KBr pellets on a Nicolet 210 spectrometer or as liquid (solvent CH_2Cl_2) on a Perkin–Elmer Spectrum One spectrometer. Chromatographic purifications were conducted by using 40–63/63–200 μm silica gel or aluminum oxide 90 standardized obtained from Merck. Thin-layer chromatography (TLC) was performed on silica gel or aluminum oxide plates (Merck) coated with fluorescent indicator. All mixtures of solvents are given in v/v ratio. The solvents used for photo-

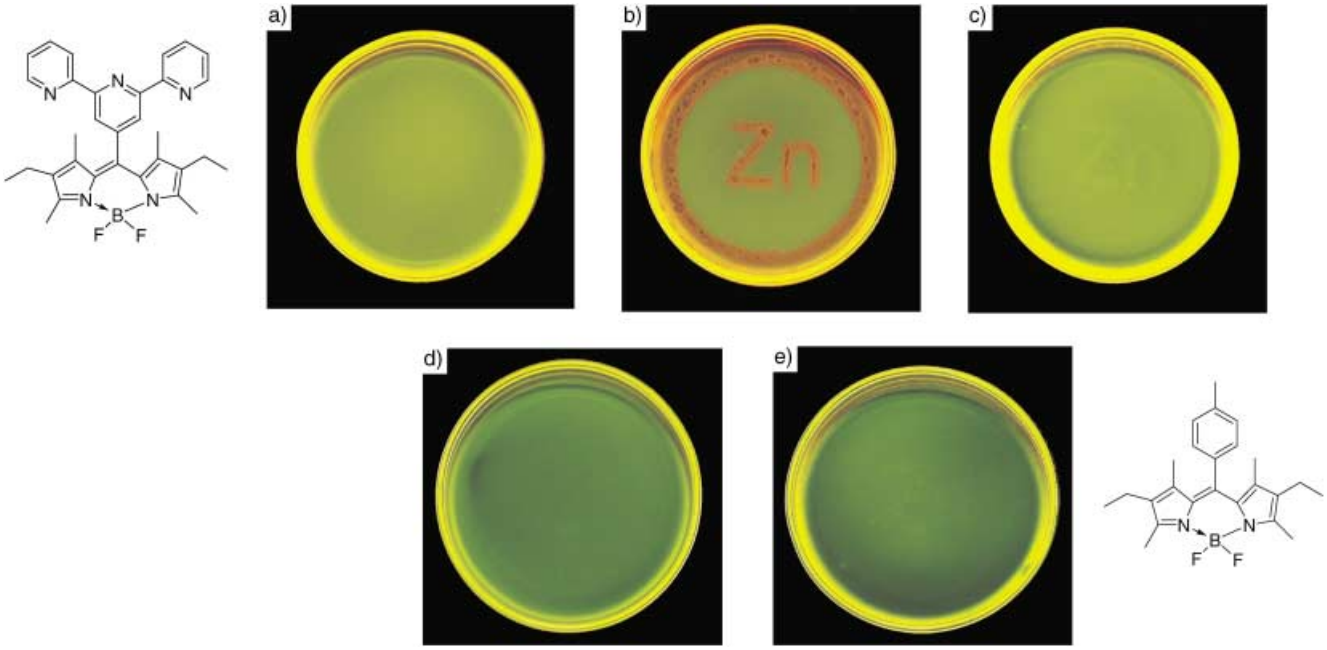

Figure 7. Fluorescence image of polymethylmethacrylate polymeric matrices impregnated with BODITERPY-**2** (top panels) or 8-*p*-tolyl-BODIPY (bottom panels). Views a) and d) refer to the polymeric dispersion of the dyes; b) and e) show the effects caused by spraying with Zn^{2+} ions; while c) shows the effect of stepwise spraying with Zn^{2+} ions and triethylenetetramine.

physical measurements were spectroscopic grade dichloromethane and acetonitrile, used without further purification. UV/Vis spectra were recorded on a Uvikon 933 spectrophotometer. Excitation and emission spectra were recorded on a Perkin Elmer LS50 B spectrofluorimeter. Luminescence quantum yields were measured in dichloromethane using Rhodamine 6G in water as reference ($\phi = 0.76$).[21] Luminescence lifetimes were measured on a PTI QuantaMaster spectrofluorimeter.

Cyclic voltammetric studies were carried by using a conventional 3-electrode set-up on a BAS CV-50W voltammetric analyser equipped with a Pt microdisc working electrode and a platinum wire counter electrode. A platinum wire soaked in acetonitrile containing the supporting electrolyte is used as pseudo reference electrode. Ferrocene was used as an internal standard and was calibrated against a saturated calomel reference electrode (SCE) separated from the electrolysis cell by a glass frit presoaked with electrolyte. Solutions contained the electroactive substrate in deoxygenated anhydrous acetonitrile containing tetra-*n*-butylammonium tetrafluoroborate (0.1M) as supporting electrolyte. The quoted half-wave potentials were reproducible to within 10 mV.

4,4-Difluoro-8-(6‴-methyl-2′:2″;6″:2‴-terpyridin-6′-yl)-1,3,5,7-tetramethyl-2,4-diethyl-4-bora-3a,4a-diaza-*s*-indacene (1): A mixture of 6-formyl-6″-methyl-2:2′;6′:2″-terpyridine[23] (0.125 g, 0.45 mmol), kryptopyrrole (135 μL, 0.99 mmol), and trifluoroacetic acid (35 μL) in anhydrous CH_2Cl_2 (50 mL) was stirred at room temperature during one week. DDQ (107 mg, 0.49 mmol) was added and the solution was stirred for 4 h. The solvent was removed and the residue was filtered on Al_2O_3 (CH_2Cl_2/methanol 99:1). The dipyrromethene was then dissolved in degassed toluene and triethylamine was added (250 μL, 1.8 mmol). After two minutes $BF_3 \cdot Et_2O$ (210 μL, 1.7 mmol) was added dropwise to the solution and the mixture was heated at 80 °C for 6 h. The mixture was then washed with a 10% aqueous $NaHCO_3$ solution, the organic layer dried over $MgSO_4$, and the solvent was evaporated. Chromatography on Al_2O_3 (CH_2Cl_2/hexane, with a gradient from 2:8 to 4:6) afforded the desired compound as a red powder (20 mg, 8%). ^{1}H NMR ($CDCl_3$): $\delta = 0.99$ (t, $^3J = 7.5$ Hz, 6H), 1.29 (s, 6H), 2.31 (q, $^3J = 7.5$ Hz, 4H), 2.56 (s, 6H), 2.67 (s, 3H), 7.22 (d, $^3J = 7.5$ Hz, 1H), 7.45 (dd, $^3J = 7.5$ Hz, $^4J = 1.0$ Hz, 1H), 7.77 (t, $^3J = 7.5$ Hz, 1H), 7.92 (t, $^3J = 8.0$ Hz, 1H), 7.99 (t, $^3J = 8.0$ Hz, 1H), 8.45 (d, $^3J = 8.0$ Hz, 1H), 8.48 (dd, $^3J = 8.0$ Hz, $^4J = 1.0$ Hz, 1H), 8.51 (dd, $^3J = 8.0$ Hz, $^4J = 1.0$ Hz, 1H), 8.78 ppm (dd, $^3J = 8.0$ Hz, $^4J = 1.0$ Hz, 1H); ^{13}C{^{1}H} NMR ($CDCl_3$): $\delta =$ 11.9 (CH_3), 13.0 (CH_3), 15.0 (CH_3), 17.5 (CH_2), 25.1 (CH_3), 118.5 (CH), 121.3 (CH), 121.6 (CH), 121.9 (CH), 123.8 (CH), 124.8 (CH), 131.2, 133.2, 137.4 (CH), 138.0, 138.1 (CH), 138.3, 138.4 (CH), 154.4, 154.9, 155.0, 155.9, 156.2, 157.0, 158.4 ppm; ^{11}B NMR ($CDCl_3$): $\delta = 3.93$ ppm (t, $J_{B,F} = 32.7$ Hz); UV/Vis (CH_2Cl_2, 23 °C): λ_{max} (ε, $M^{-1}cm^{-1}$) = 288 (42800), 529 ppm (67000); FAB^+/MS (*m*-NBA): *m*/*z* (%): 550 (100) [M^++H]; elemental analysis calcd (%) for $C_{33}H_{34}BF_3N_5$: C 72.13, H 6.24, N 12.75; found: C 71.85, H 5.93, N 12.54.

4,4-Difluoro-8-(2′:2″;6″:2‴terpyridin-4″-yl)-1,3,5,7-tetramethyl-2,4-diethyl-4-bora-3a,4a-diaza-*s*-indacene (2): A solution of 4′-formyl-2′:2″;6″:2‴-terpyridine (0.5 g, 1.9 mmol), 2,4-dimethyl-3-ethylpyrrole (570 μL, 4.2 mmol) and trifluoroacetic acid (150 μL) in dry CH_2Cl_2 was stirred at room temperature during one week. DDQ (0.42 g, 1.93 mmol) was added and the solution stirred for 4 h. The solution was washed with a saturated aqueous solution of $NaHCO_3$ and the organic layer dried over $MgSO_4$. A short chromatography column (Al_2O_3, CH_2Cl_2/MeOH 99:1) was used to purify the free indacene. This intermediate was dissolved in toluene (200 mL), triethylamine (500 μL) and $BF_3 \cdot Et_2O$ (350 μL, 2.8 mmol) were added to the solution. The solution turned red immediately and was allowed to stir one day at room temperature. The slurry was washed with a saturated aqueous solution of $NaHCO_3$, the organic layer was dried and chromatography (Al_2O_3, gradient CH_2Cl_2/hexane 20:80 → 50:50) afforded the title compound as a red powder (0.73 g, 73%). ^{1}H NMR ($CDCl_3$): δ 0.96 (t, $^3J =$ 7.5 Hz, 6H), 1.43 (s, 6H), 2.28 (q, $^3J = 7.5$ Hz, 4H), 2.55 (s, 6H), 7.52 (ddd, $J = 7.5$ Hz, $J = 4.6$ Hz, $J = 1.2$ Hz, 2H), 7.90 (td, $^3J = 7.8$ Hz, $^5J = 1.8$ Hz, 2H), 8.54 (s, 2H), 8.66–8.72 ppm (m, 4H); ^{13}C{^{1}H} JMOD NMR ($CDCl_3$): $\delta =$ 12.7 (CH_3), 14.4 (CH_3) 14.8 (CH_3), 17.5 (CH_2), 121.1 (CH), 122.3 (CH), 123.7 (CH), 131.5, 134.0, 134.4, 135.1, 136.8 (CH), 149.1, 149.2 (CH), 150.5, 155.6, 155.9 ppm; ^{11}B NMR ($CDCl_3$): $\delta = 3.86$ ppm (t, $J_{B,F} = 32.75$ Hz); UV/Vis (CH_2Cl_2, 23 °C): λ_{max} (ε, $M^{-1}cm^{-1}$) = 239 (38500), 279 (25700), 376 (8400), 529 nm (72000); IR (KBr): $\tilde{\nu} = 3445$ (m), 2926 (s), 1743 (m, $\nu_{C=N}$), 1542 (s), 1465 (s), 1190 cm^{-1} (s); FAB^+-MS (*m*-NBA): *m*/*z* (%): 536.2 (100) [M^++H]; elemental analysis calcd (%) for $C_{32}H_{32}N_5BF_3$: C 71.78, H 6.02, N 13.08; found: C 71.64, H 5.94, N 12.97.

UV/Vis and fluorescence titration experiments: In a typical experiment, 2 mL of a solution of the ligand (concentration varying from 1×10^{-5} to 3×10^{-5}M) dissolved in non-degassed distilled acetonitrile containing 0.01M tetrabutylammoniumhexafluorophosphate (TBAH) as an inert salt was titrated by increasing aliquots of a solution of the metal ($c = 7 \times 10^{-5}$ to 1.5×10^{-4}M) as their perchlorate salts in the same solvent. After each added aliquot the UV/Vis spectrum of the solution was recorded at 298 ± 2 K by using 1 cm path length quartz cells. The relative concentrations of the ligands and the metals were chosen so as to obtain a final metal-to-ligand ratio of 5 to 10 equivalents. Absorption spectra were measured from 240 to

600 nm at one point per nm with the total number of spectra varying from 18 to 29 per experiment. The spectra were then implemented in the Specfit software.[24] Factorial analysis of the titration data together with optical density variations at varying wavelengths gave a preliminary insight into the number of new absorbing species and their stoichiometric coefficients. According to this, a model was proposed in which the different formed species were introduced in the form given in expression (1).

$$x\,M^{n+} + y\,L \leftrightarrow [M_xL_y]^{nx+} \qquad \beta_{xy} = [M_xL_y{}^{nx+}]/([L]^y \cdot [M^{n+}]^x) \tag{1}$$

Where β_{xy} refers to the conditional cumulative stability constant for formation of the complex with x metal atoms and y ligands. The experimental data were then fitted to the model with nonlinear least squares algorithms and the calculated β_{xy} values were retained when the model had converged with maximum deviations smaller than 5% between calculated and measured absorbances for all the points of the experiments. The $\log\beta_{xy}$ values given in the text are the average of at least two titration experiments in which starting concentrations have been varied. The estimated error is the average value of the error obtained from each measurement. In the case of zinc, the presence of an isosbestic point at 315 nm in the absorption titration experiment was used to simplify the fitting process for fluorescence titration. The excitation wavelength was thus chosen at 315 nm considering that all the species formed have the same molar extinction coefficient per number of ligands (x). Considering that the total emitted intensity is then a linear combination of the concentrations of the species present multiplied by their respective quantum yields, the titrations were fitted according to the procedure described above. Corrections for auto-absorption and instrumental response[25] were not taken into account.

Formation of the polymer films: The samples were prepared in Pétri dishes (7 cm in diameter), containing polymethylmethacrylate polymer (280 mg; $M_w = 95\,000$, $M_n = 65\,000$) dissolved in prefiltered dichloromethane (28 mL) and doped with BODITERPY **2** (1.4 mg, 0.5 wt%). The Pétri dishes were covered with a top and the solvent slowly evaporated to dryness under a well ventilated hood. After two days the transparent and homogeneous thin film was recovered with a shadow mask (5.5 cm in diameter) including the fingerprint (in our case Zn). Then a solution containing zinc perchlorate in acetonitrile (10^{-3} M) was sprayed onto the film and the solvent was allowed to evaporate in air for 1 h. To take the picture the mask was withdrawn. For the second step (erasing process) the mask was centered again over the film and the competitor (triethylenetetramine in acetonitrile) was pulverized under the same conditions as previously described.

Crystal structure determination of ligand 1: The X-ray diffraction data on a single microcrystal were recorded at the DW-32 station on the wiggler line at the synchrotron DCI (Orsay), using a MAR 345 image plate system at $\lambda = 0.964$ Å.[26] More than a full 360° rotation range was recorded (80 frames, 5° rotation each). Owing to the geometric restrictions, the resolution at the edge of the detector was reduced to 1.01 Å. Data reductions were done using the DENZO program from the HKL suite.[27] This allowed the integration of 38 952 reflections which were subsequently reduced to 2955 independent reflections including systematic absences ($R_{merge} = 0.049$) and formatted in a suitable form for the SHELXL suite of programs.[28] The final data set consists of 2755 unique reflections of which 2433 are considered as observed (with $F_o \geq 2\sigma F_o$). The structure was solved by direct methods (SHELX-S86)[29] and was refined on F^2 for all reflections by least-squares methods using SHELXL-93.[28] All hydrogen atoms were located on difference-Fourier syntheses. They were modeled at their theoretical positions ($C-H_{ar} = 0.93$ Å, $C-H_{Me} = 0.96$ Å) using an isotropic thermal factor equal to 1.2 times that of the bonded atom and introduced in the refinement cycles. The final conventional R value is 0.0504 for 2433 observed reflections with $F_o > 2\sigma F_o$ and 377 parameters, and 0.0548 for all data, $wR(F^2) = 0.15$ for all, $w = 1/[\sigma^2 F_o^2 + (0.1007P)^2 + 1.03P]$, where $P = (F_o^2 + 2F_c^2)/3$. The largest difference peak and hole are 0.16 and -0.17 e Å^{-3}. A summary of the crystallographic data is given in Table 3.

CCDC-201034 contains the supplementary crystallographic data for this paper. These data can be obtained free of charge via www.ccdc.cam.ac.uk/conts/retrieving.html (or from the Cambridge Crystallographic Data Centre, 12 Union Road, Cambridge CB2 1EZ, UK; fax: (+44) 1223-336033; or deposit@ccdc.cam.uk).

Table 3. Crystallographic data for ligand **1**.

formula	$C_{33}H_{34}BF_2N_5$
M_r	549.46
crystal system	monoclinic
space group	$P21/n$
a [Å]	17.128(1)
b [Å]	9.325(1)
c [Å]	18.109(1)
β [°]	91.53(3)
V [Å^3]	2891(3)
Z	4
λ [Å]	0.964
$F(000)$	1160
ρ_{calcd} [Mg m^{-3}]	1.262
$\mu(Mo_{K\alpha})$ [mm^{-1}]	0.084
crystal size [mm]	$0.05 \times 0.03 \times 0.01$
T [K]	177(2)
reflections measured	38952
θ range	$2.19 < 2\theta < 28.96$
hkl ranges	$0 \leq h \leq 16$
	$0 \leq k \leq 9$
	$-17 \leq l \leq 17$
unique reflections	2755
reflections observed $I > 2\sigma(I)$	2433
parameters/restraints	377/0
$R1[I > 2\sigma(I)]$[a] (obs/all data)	0.0504/0.0548
$wR2$[c] (obs/all data)	0.1476/0.1514
weight	$1/[\sigma^2 F_o^2 + (0.1007P)^2 + 1.03P]$
max Fourier diff [eÅ^3]	0.16, −0.17

[a] $R1 = \Sigma\,||F_o| - |F_c||/\Sigma|F_o|$. [b] $P = (F_o^2 + 2F_c^2)/3$. [c] $wR2 = \{\Sigma[w(F_o^2 - F_c^2)^2]/\Sigma[w(F_o^2)^2]\}^{1/2}$.

Acknowledgement

This work was supported by the Centre National de la Recherche Scientifique, the Université Louis Pasteur and the IST/ILO Contract-2001 – 33057.

[1] R. W. Wagner, J. S. Lindsey, *Pure. Appl. Chem*. **1996**, *68*, 1373.
[2] *Chemosensors of Ion and Molecular Recognition*, (Eds.: J.-P. Desverne, A. W. Czarnik), NATO Advanced Study Institute Series C492, Kluwer, Dordrecht, **1997**; R. P. Haugland, *Handbook of Molecular Probes and Research Products*, 9th ed., Molecular Probes, Inc., Eugene, OR, **2002**.
[3] A. P. De Silva, H. Q. N. Gunaratne, T. Gunnlaugsson, A. J. M. Huxley, C. P. McCoy, J. T. Rademacher, T. E. Rice, *Chem. Rev*. **1997**, *97*, 1515.
[4] a) M. A. Baldo, D. F. O'Brien, Y. You, A. Shoustikov, S. Sibley, M. E. Thompson, S. R. Forrest, *Nature*, **1998**, *395*, 151; b) J. H. Schon, A. Dodabalapur, C. Kloc, B. Batlogg, *Science*, **2000**, *290*, 963.
[5] a) H. Miyaji, W. Sato, J. L. Sessler, *Angew. Chem*. **2000**, *112*, 1847; *Angew. Chem. Int. Ed*. **2000**, *39*, 1777; b) P. Anzenbacher, Jr., K. Jursikova, J. L. Sessler, *J. Am. Chem. Soc*. **2000**, *122*, 9350.
[6] a) M. Hissler, A. Harriman, P. Jost, G. Wipff, R. Ziessel, *Angew. Chem*. **1998**, *110*, 3439; *Angew. Chem. Int. Ed*. **1998**, *37*, 3249; b) A. Harriman, M. Hissler, P. Jost, G. Wipff, R. Ziessel, *J. Am. Chem. Soc*. **1999**, *121*, 14.
[7] T. D. James, S. Shinkai, *Top. Curr. Chem.* **2002**, *218*, 159.
[8] P. Zhang, T. Beck, W. Tan, *Angew. Chem*. **2001**, *113*, 416; *Angew. Chem. Int. Ed*. **2001**, *40*, 402.
[9] M. Hissler, A. El-Ghayoury, A. Harriman, R. Ziessel, *Angew. Chem*. **1998**, *110*, 1804; *Angew. Chem. Int. Ed*. **1998**, *37*, 1717.
[10] L. J. Charbonnière, R. Ziessel, M. Montalti, L. Prodi, N. Zaccheroni, C. Boehme, G. Wipff, *J. Am. Chem. Soc*. **2002**, *124*, 7779.
[11] a) M. Kollmannsberger, K. Rurack, U. Resch-Genger, J. Daub, *J. Phys. Chem. A* **1998**, *102*, 10211; b) K. Rurack, M. Kollmannsberger, U. Resch-Genger, J. Daub, *J. Am. Chem. Soc*. **2000**, *122*, 968; c) B. Turfan, E. U. Akkaya, *Org. Lett*. **2002**, *4*, 2857.

[12] F. Sancenon, R. Martinez-Manez, J. Soto, *Angew. Chem*. **2002**, *114*, 1474; *Angew. Chem. Int. Ed*. **2002**, *41*, 1416.
[13] H. Fischer, P. Halbig, B. Walach, *Ann. Chem*. **1927**, *452*, 268.
[14] A. Burghart, H. Kim, M. B. Welch, L. H. Thoresen, J. Reibenspies, K. Burgess, *J. Org. Chem*. **1999**, *64*, 7813.
[15] M. Kollmannsberger, T. Gareis, S. Heinl, J. Breu, J. Daub, *Angew. Chem*. **1997**, *109*, 1391; *Angew. Chem. Int. Ed*. **1997**, *36*, 1333.
[16] T. Ohno, S. Kato, *Bull. Chem. Soc. Jpn.* **1974**, *47*, 2953; G. Albano, V. Balzani, E. C. Constable, M. Maestri, D. R. Smith, *Inorg. Chim. Acta* **1998**, *277*, 225.
[17] F. Li, S. I. Yang, Y. Ciringh, J. Seth, C. H. Martin III, D. L. Singh, D. Kim, R. R. Birge, D. F. Bocian, D. Holten, J. S. Lindsey, *J. Am. Chem. Soc*. **1998**, *120*, 10001.
[18] The lower limit was obtained on a routine Perkin Elmer LS 50 Spectrofluorimeter by measuring the decrease of luminescence intensity upon addition of one equivalent of $Zn(ClO_4)_2$ to a solution of ligand **2**. This operation was repeated with gradually diluted solutions until less than 50% of the signal was lost, resulting in a lower limit of 5×10^{-7} M.
[19] A. Sarkar, S. Chakravorti, *J. Lumin.* **1995**, *63*, 143; W. Goodall, J. A. Williams, *Chem. Commun*. **2001**, 2514.
[20] M. Schütz, R. Schmidt, *J. Phys. Chem.* **1996**, *100*, 2012.
[21] J. Olmsted III, *J. Phys. Chem.* **1979**, *83*, 2581.
[22] J.-P. Collin, A. Harriman, V. Heitz, F. Odobel, J.-P. Sauvage, *J. Am. Chem. Soc.* **1994**, *116*, 5679.
[23] G. Ulrich, unpublished results.
[24] H. Gammp, M. Maeder, C. J. Meyer, A. D. Zuberbühler, *Talanta* **1985**, *32*, 257.
[25] A. Credi, L. Prodi, *Spectrochim. Acta A* **1998**, *54*, 159.
[26] R. Fourme, P. Dhez, J. P. Benoit, R. Kahn, J. M. Dubuisson, P. Besson, J. Frouin, *Rev. Sci. Instrum.* **1992**, *63*, 982.
[27] Z. Otwinowski, W. Minor, *Methods Enzymol.* **1997**, *276*, 307.
[28] SHELXL, G. M. Sheldrick, "Program for the Refinement of Crystal Structures", University of Göttingen, Germany, **1993**.
[29] G. M. Sheldrick, *Acta Crystallogr. Sect A* **1990**, *46*, 467.

Received: April 15, 2003 [F5084]

